JOURNAL OF SOLID STATE CHEMISTRY 96, 115–122 (1992)

Elementary Formulation of the Verwey Transition in Magnetite via the Order–Disorder Formalism

J. M. HONIG* AND J. SPAŁEK†

* *Department of Chemistry, Purdue University, West Lafayette, Indiana 47907-1393 and †Institute of Theoretical Physics, University of Warsaw, ul. Hoża 69, PL-00681 Warsaw, Poland*

Received July 29, 1991

DEDICATED TO PROFESSOR PAUL HAGENMULLER ON HIS 70th BIRTHDAY

A review of experimental data relating to the Verwey transformation in $Fe_{3(1-\delta)}O_4$ and in $Fe_{3-x}Zn_xO_4$ is presented. The transition from first order to higher order with increasing δ or x is rationalized by representing the host crystal in terms of octahedral site pairs that share electrons between the two sites. The individual octahedral interstices can remain unoccupied or become occupied by localized or itinerant electrons. The application of the order-disorder formalism leads to the construction of a free energy expression which must be optimized. If the resulting relations are simplified by adopting energy parameters associated with several limiting cases, one automatically obtains the model of Strässler and Kittel. This theory had previously been demonstrated to be very useful in rationalizing both the thermodynamic and the transport properties of magnetite. © 1992 Academic Press, Inc.

1. Introductory Comments

The phase transition in magnetite has been the subject of a large number of studies ever since the original report by Millar (*1*) of a heat-capacity anomaly near 120 K. A further impetus was provided by Verwey (*2*), who reported a concomitant electrical-resistivity anomaly in that temperature range. Although it was clear from Verwey's studies that the oxygen/metal ratio in magnetite plays a crucial role in the detailed manifestations of the phase transformation, this feature remained largely unappreciated by later workers. For this reason much of the work reported in the literature has failed to clarify the underlying issues pertaining to the Verwey transition. At a later stage the research by Dieckmann and Schmalzried (*3, 4*) and by Gmelin and co-workers (*5*) involved detailed and careful studies of variations in oxygen stoichiometry and their effects on the physical properties of magnetite. However, it was not until very recently that a new feature was uncovered (*6–13*), namely, that the Verwey transition in $Fe_{3(1-\delta)}O_4$ was of first order in the range $-0.0005 \le \delta < \delta_c \equiv 0.0039$, and of second order in the range $\delta_c < \delta < 3\delta_c$. This was established through magnetization, thermodynamic, electrical, structural, and Mössbauer studies on single crystals of high purity that had been carefully annealed in a CO/CO_2 buffering atmosphere. Attempts to

0022-4596/92 $3.00

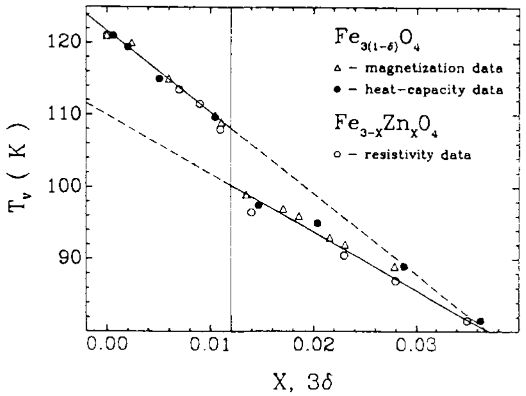

FIG. 1. Variation of the Verwey transition temperature with 3δ in $Fe_{3(1-\delta)}O_4$ and with x in $Fe_{3-x}Ti_xO_4$.

work with materials in the range $\delta > 3\delta_c$ proved unsuccessful because of the proximity of the magnetite–hematite phase boundary. Similar results have recently been reported (*14–16*) for the $Zn_xFe_{3-x}O_3$ system, with the correspondence $x = 3\delta$, except that it is obviously now possible to explore the composition region $x > 3\delta_c$, where the Verwey transition was found to disappear altogether. These various results are summarized in Fig. 1, which shows a plot of the Verwey transition temperature T_V in $Fe_{3(1-\delta)}O_4$ and in $Fe_{3-x}Zn_xO_4$ vs. 3δ or x, as determined by various experimental techniques detailed in the figure legend. Departures from the parent composition Fe_3O_4 lead to a steady decrease in T_V; one can see the domain of first and second order transitions and the cutoff beyond which $Fe_{3-x}Zn_xO_4$ fails to show any transitions at all. As a further illustration of these phenomena we exhibit in Fig. 2 a plot of log ρ vs $1/T$ for $Fe_{3(1-\delta)}O_4$ and $Fe_{3-x}Zn_xO_4$, where ρ is the resistivity and T is the temperature. The $x = 3\delta$ correspondence in the electrical resistivities, which are representative of other physical properties, is very striking. This feature is consistent with the designations $Zn_{x/3}Fe_{1-x/3}O_{4/3}$ and $Fe_{1-\delta}O_{4/3}$ for zinc-doped and nonstoichiometric magnetite relative to the ideal $FeO_{4/3}$ composition per mole of iron. A proper justification of the $x = 3\delta$ relation involves elementary but lengthy arguments that are presented elsewhere (*17*).

In what follows we attempt to provide a simple framework model for the rationalization of the observed alteration in the character of the Verwey transition with doping by vacancies or by zinc. The present exposition generalizes earlier preliminary analyses (*18, 19*): a more detailed interpretation is still in the early stages of development.

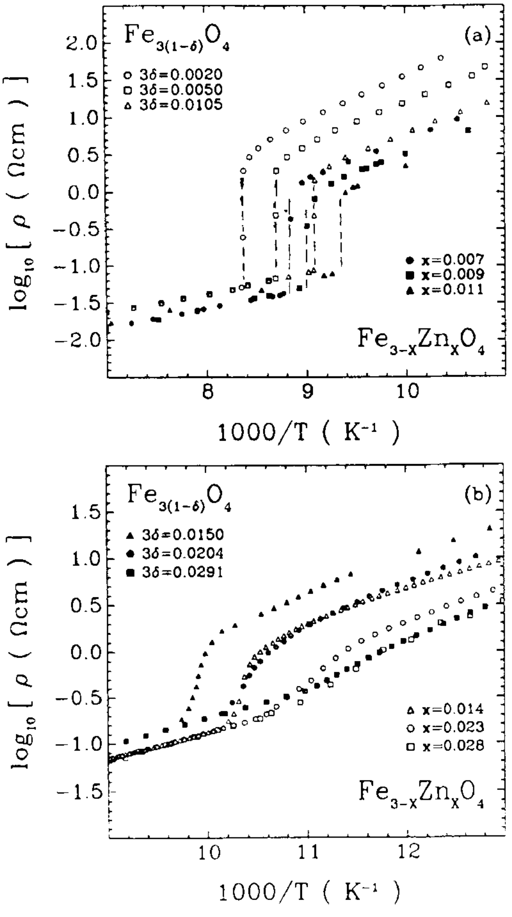

FIG. 2. Logarithm of resistivity (in ohm-cm) vs. reciprocal temperature (K) for $Fe_{3(1-\delta)}O_4$ and $Fe_{3-x}Zn_xO_4$.

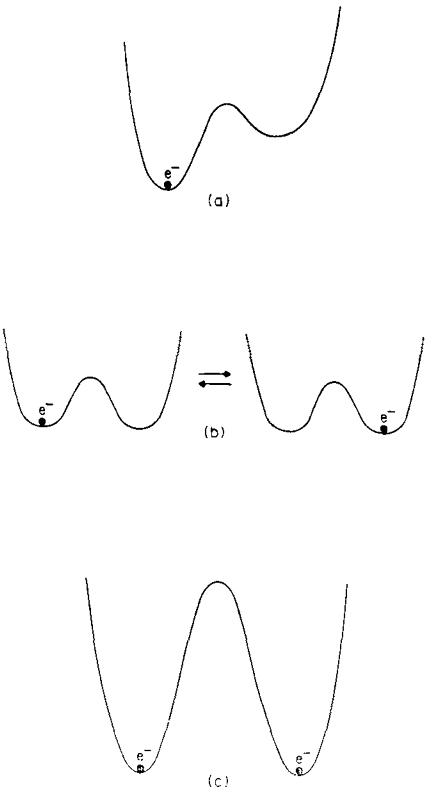

FIG. 3. Site occupancies in bond representation of Fe_3O_4 lattice: (a) Ground state of distorted lattice. (b) Resonant energy configuration; precursor to directed drift of carriers in an applied field. (c) Double occupancy of octahedral site pair.

At the outset we focus on the important role played by the octahedral site pairs. Consider the cation distribution in $(Zn_x^{2+}, Fe_{1-x}^{3+})[Fe_{1-x}^{2+}, Fe_{1+x}^{3+}]O_4$ and in $(Fe^{3+})[Fe_{1-9\delta}^{2+}Fe_{1+6\delta}^{3+}]O_4$, where the units in round and square brackets denote ions located in tetrahedral (t) and octahedral (o) sites respectively. Those on t locations are not subject to valence fluctuations; those on o locations can be considered as basically pairs of Fe^{3+} ions sharing an extra electron that can respond to external fields or to temperature changes. This argument focuses on the importance of octahedrally coordinated pairs of interstitial sites for rationalizing the observed electronic properties of magnetite, including the Verwey transition. Clearly, for the case where every Fe^{2+} is surrounded by Fe^{3+} units and vice versa the energy of the system is minimized; however, this also represents the case of lowest entropy. As usual, the physical characteristics of the system are then determined by the balance between these two opposing tendencies, as specified by the global minimum in the free energy. We now examine this situation in further detail.

2. The Order–Disorder Formalism as a Model for the Magnetite System

The preceding remarks make plausible the use of pairs of octahedral sites as a very rudimentary representation of magnetite. We simplify further by neglecting configurations arising from the presence of the very low concentrations of Zn^{2+} or of cation vacancies.

Three possible configurations for occupation of o–o site pairs are shown in Fig. 3 and in Table I. Relative to the "vacuum configuration" [Fe^{3+}, Fe^{3+}], the ground state (Fig. 3a) is that in which an extra electron is localized at one of the two o sites, surrounded by a deep potential well. This incurs a distortion of the type involved in

TABLE I

LATTICE REPRESENTATION

Configurations			Probability	Energy
		Bond representation		
●	●	BB	β_2	ε_{BB}
●	○	BA	$2\beta_1$	ε_{BA}
○	●	AB		ε_{AB}
⊗	○	CA	β_0	ε_{CA}
		Site representations		
●		B	γ_2	ε_2
○		A	γ_1	ε_1
⊗		C	γ_0	ε_0

the phase transition from the cubic spinel ($T > T_V$) to the monoclinic ($T < T_V$) phase. A second state (Fig. 3b) of higher energy involves the extra charge carrier in an undisturbed site, where it has access to either location with equal probability. This resonant state is the precursor to the directed drift of the carrier under the influence of an external electric field. The state of highest energy (Fig. 3c) is that in which two mobile charge carriers occupy two adjacent o sites; these carriers cannot move toward each other but can proceed to other adjacent empty sites. In accordance with the above scheme we define β_0, $2\beta_1$, and β_2 as the probability of encountering o–o site pairs in the configurations CA, AB or BA, and BB, with energies ε_{CA}, $\varepsilon_{AB} = \varepsilon_{BA}$, and ε_{BB} respectively. The entries are exhibited in detail in Table I, part A.

The possible occupation states of individual sites are shown in Table I, part B. There are three possibilities. A fraction γ_0 of the o-sites is occupied by electrons trapped through lattice deformations; the corresponding energy is ε_0. A fraction $\gamma_1 \equiv c_1$ is unoccupied; this quantity is fixed through the parameters δ or x characterizing the composition of the solid. The corresponding energy is ε_1. A fraction $\gamma_2 \equiv \alpha_1$ represents sites containing mobile carriers; this quantity in principle is accessible experimentally via resistivity or Seebeck coefficient measurements. The corresponding energy is ε_2.

The six parameters β_j and γ_i in Table I are not independent. First, one must take account of the normalization requirements

$$\beta_2 + 2\beta_1 + \beta_0 = 1 \qquad (2.1)$$

$$\gamma_2 + \gamma_1 + \gamma_0 = 1. \qquad (2.2)$$

In addition one must adopt the consistency condition for mobile charge carriers, which is derived as follows: In the bond and site representations there are a total of $(Z/2)L(2\beta_1 + 2\beta_2) + (1 - Z)L\gamma_2$ carriers that can respond to the imposition of an external field. In the real lattice that number is $L\gamma_2$. These two quantities must match; this leads to the consistency requirement

$$\beta_2 + \beta_1 = \gamma_2 \equiv \alpha_1. \qquad (2.3)$$

Finally, one should note again the requirement that the composition of the samples be fixed, so that

$$\gamma_1 = c_1, \qquad (2.4)$$

where c_1 is the fraction of o-sites that do not contain any extra electrons, whether mobile or frozen.

Thus, the number of independent variables is reduced from six to two. We select β_1 and γ_2 as the independent set, thereby focusing on the number of electrons that can respond to the applied external field. It is also expedient to rewrite Eqs. (2.1) and (2.3) as

$$\beta_2 = \gamma_2 - \beta_1, \quad \beta_0 = 1 - \gamma_2 - \beta_1. \qquad (2.5)$$

3. Mathematical Development

On the basis of the probability variables and energy parameters introduced earlier it is straightforward to construct the energy and entropy for the representative figure assemblies.

The energy of the bond assembly is given by

$$E_b = \frac{Z}{2}L(\beta_2\varepsilon_{BB} + 2\beta_1\varepsilon_{AB} + \beta_0\varepsilon_{CA})$$
$$= \frac{Z}{2}L(\beta_2 U + 2\beta_1\varepsilon + \varepsilon_{CA}), \qquad (3.1)$$

where

$$U \equiv \varepsilon_{BB} - \varepsilon_{CA} = U(\beta_2), \quad \text{and}$$
$$\varepsilon \equiv \varepsilon_{AB} - \varepsilon_{CA} = \varepsilon(\beta_1). \qquad (3.2)$$

One should note that U and ε are taken to be functions of β_2 and β_1, respectively. U' and ε', introduced below, are derivatives with respect to the appropriate variable.

The energy for the site assembly is

$$\begin{aligned} E_s &= (1 - Z)L(\gamma_2\varepsilon_2 + \gamma_1\varepsilon_1 + \gamma_0\varepsilon_0) \\ &= (1 - Z)L(\gamma_2\varepsilon_B + \gamma_1\varepsilon_A + \varepsilon_0), \end{aligned} \tag{3.3}$$

where

$$\varepsilon_B \equiv \varepsilon_2 - \varepsilon_0, \quad \varepsilon_A \equiv \varepsilon_1 - \varepsilon_0. \tag{3.4}$$

In Stirling's approximation the entropy for the bond assembly is specified by

$$\begin{aligned} S_b = -k_B\frac{Z}{2}L(\beta_2 \ln\beta_2 \\ + 2\beta_1 \ln\beta_1 + \beta_0 \ln\beta_0), \end{aligned} \tag{3.5}$$

where k_B is Boltzmann's constant. The entropy of the site assembly is

$$\begin{aligned} S_s = -k_B(1 - Z)L(\gamma_2 \ln\gamma_2 \\ + \gamma_1 \ln\gamma_1 + \gamma_0 \ln\gamma_0). \end{aligned} \tag{3.6}$$

We now assemble (3.1), (3.3), (3.5), (3.6) to obtain the Helmholtz free energy function

$$\begin{aligned} F &= E_b + E_s - TS_b - TS_s \\ &= \frac{Z}{2}L[\beta_2 U + 2\beta_1\varepsilon + \varepsilon_{CA}] \\ &\quad + (1 - Z)L[\gamma_2\varepsilon_B + \gamma_1\varepsilon_A + \varepsilon_0] \\ &\quad + k_B T\frac{Z}{2}L[\beta_2 \ln\beta_2 + 2\beta_1 \ln\beta_1 + \beta_0 \ln\beta_0] \\ &\quad + k_B T(1 - Z)L(\gamma_2 \ln\gamma_2 + \gamma_1 \ln\gamma_1 + \gamma_0 \ln\gamma_0). \end{aligned} \tag{3.7}$$

Eq. (3.7) must then be optimized with respect to β_1:

$$\begin{aligned} \frac{dF}{d\beta_1} = 0 = \frac{Z}{2}L\bigg[\beta_2 U'\frac{d\beta_2}{d\beta_1} + U\frac{d\beta_2}{d\beta_1} + 2\varepsilon \\ + 2\beta_1\varepsilon'\bigg] + k_B T\frac{Z}{2}L\bigg[(\ln\beta_2)\left(\frac{d\beta_2}{d\beta_1}\right) + \frac{d\beta_2}{d\beta_1} \\ + 2\ln\beta_1 + 2 + (\ln\beta_0)\left(\frac{d\beta_0}{d\beta_1}\right) + \frac{d\beta_0}{d\beta_1}\bigg]. \end{aligned} \tag{3.8}$$

The above relation may be rearranged as

$$\begin{aligned} \ln\left(\frac{\beta_2\beta_0}{\beta_1^2}\right) = \frac{-1}{k_B T}\Big\{(U - 2\varepsilon) - \beta_2 U' \\ - 2\beta_1\varepsilon'\Big\} \equiv \frac{-R}{k_B T}, \end{aligned} \tag{3.9}$$

or as

$$\beta_2\beta_0/\beta_1^2 = \exp(-R/k_B T) \equiv C. \tag{3.10}$$

Eq. (3.10) may be solved for β_1 by introducing Eqs. (2.5). One obtains a quadratic form in β_1 with the solution

$$\begin{aligned} \beta_1 &= \\ &\frac{1}{2(1 - C)}\left\{1 - \sqrt{1 - 4(1 - C)\alpha_1(1 - \alpha_1)}\right\}, \end{aligned} \tag{3.11}$$

where the positive sign ahead of the square root was discarded to render $\beta_1 \leq 1$. Note that β_2 and β_0 in Eq. (2.5) are now functions of α_1 alone.

Eqs. (2.5) may next be introduced into Eq. (3.7) to substitute for the multipliers of the logarithmic terms involving β_0 and β_2. On subsequently collecting terms one obtains an expression in which the quantity $\beta_1 \ln(\beta_0\beta_2/\beta_1^2)$ may be eliminated by use of Eq. (3.9). After further simplification one obtains the optimized function

$$\begin{aligned} F_{\beta 1} = \frac{Z}{2}L[\beta_1 U + \beta_1(\gamma_1 - \beta_1)U' \\ - 2\beta_1^2\varepsilon' + \varepsilon_{CA}] + (1 - Z)L[\gamma_2\varepsilon_B \\ + \gamma_1\varepsilon_A + \varepsilon_0] + \frac{Z}{2}Lk_B T[\gamma_2 \ln\beta_1 \\ + (1 - \gamma_2)\ln(1 - \gamma_2 - \beta_1)] \\ + k_B T(1 - Z)L[\gamma_2 \ln\gamma_2 + \gamma_1 \ln\gamma_1 \\ + (1 - \gamma_1 - \gamma_2)\ln(1 - \gamma_1 - \gamma_2)], \end{aligned} \tag{3.12}$$

which makes no reference to the parameter ε.

As a last step one must enforce equilibrium by optimizing Eq. (3.12) through the condition $dF_{\beta_1}/d\gamma_2 = 0$. Account must be taken of the dependence of the β_j variables on γ_2. The resulting expression furnishes

TABLE II

SPECIAL CASES BASED ON EQS. (2.5) AND (3.9)

(A) $C = 0$	(B) $C = 1$	(C) $C \to \infty$
$\beta_2 = 0$	$\beta_2 = \gamma_2^2$	$\beta_2 = \gamma_2$
$\beta_1 = \gamma_2$	$\beta_1 = \gamma_2(1 - \gamma_2)$	$\beta_1 = 0$
$\beta_0 = 1 - \gamma_2$	$\beta_0 = (1 - \gamma_2)^2$	$\beta_0 = 1 - \gamma_2$

an interrelation which may be used to convert Eq. (3.12) into a function $F_{\beta_1\gamma_2} = F_{\beta_1\gamma_2}(\gamma_2; \gamma_1, T)$ from which β_1 has been eliminated. These mathematical steps are lengthy though not difficult; however, they tend to obscure the points on which we wish to focus. We therefore adopt simplifying approximations discussed in the next section.

4. Special Cases

Before turning to special cases we note that Eq. (3.9), which specifies the optimal set of β_j, makes no direct reference to the properties of the $(1 - Z)L$-member point figure assembly whose properties are not needed here. Hence we treat the bond–figure assembly as the particular item of interest and we therefore concentrate on the properties of the $(ZL/2)$ site pairs required to represent one mole of Fe_3O_4. The corresponding free energy may be found by returning to Eqs. (3.1) and (3.5) and writing

$$\tilde{F}_b = [\beta_2 U + 2\beta_1 \varepsilon + \varepsilon_{AA}] + k_B T(\beta_2 \ln \beta_2 + 2\beta_1 \ln \beta_1 + \beta_0 \ln \beta_0). \quad (4.1)$$

For this special situation we adopt the limits $C = 0, 1, \infty$ in Eq. (3.10). Eqs. (2.1), (2.3), and (4.1) then simplify to the special results shown in Table II. We consider each of these in turn:

(A) $C = 0$, under the sufficient condition $U \to \infty$; since $\beta_2 = 0$ for large but finite U, $\beta_2 U = 0$, and U' can be ignored. Equation (3.12) now reduces to

$$\tilde{F}_{\beta_1} = 2\beta_1 \varepsilon + \varepsilon_{CA} + k_B T[2\beta_1 \ln \beta_1 + (1 - 2\beta_1)\ln(1 - 2\beta_1)]. \quad (4.2)$$

At this point it is useful to introduce the order parameter $\psi \equiv 2\beta_1 \equiv 2\gamma_2$; since $\gamma_2 \leq 1 - c_1 \leq \frac{1}{2}$ the order parameter lies in the range $0 \leq \psi \leq 1$. Then

$$\tilde{F}_{\beta_1} = \psi\, \varepsilon(\psi) + \varepsilon_{CA} + k_B T[\psi \ln \psi + (1 - \psi)\ln(1 - \psi) - \psi \ln 2]. \quad (4.3)$$

Optimization with respect to ψ via $\partial \tilde{F}_{\beta_1}/\partial \psi = 0$ yields the expression

$$\frac{\varepsilon(\psi) + \psi\, \varepsilon'(\psi)}{k_B T} = -\ln\left(\frac{\psi}{1 - \psi}\right) + \ln 2. \quad (4.4)$$

One should note that Eq. (4.3) is formally equivalent to the free energy of a binary solution consisting of components with mole fractions ψ and 1-ψ; the extra contribution arising from the term ψ ln 2 will later turn out to be crucial. The condition $U \to \infty$ has reduced the three-level problem to a two-level case.

(B) $C = 1$, under the sufficient condition that $U = 2\varepsilon$ and $U' = \varepsilon' = 0$. From Table II and Eq. (4.1) one now obtains the result $(\gamma_2 \equiv \alpha_1)$

$$\tilde{F}_{\beta_1} = 2\varepsilon\alpha_1 + \varepsilon_{CA} + 2k_B T\{\alpha_1 \ln \alpha_1 + (1 - \alpha_1)\ln(1 - \alpha_1)\}. \quad (4.5)$$

In this manner the original three-level problem has again been converted to an equivalent quasi-two-level problem in which the order parameter is now given by $\psi = \alpha_1$, $0 \leq \psi \leq 1$. Again, this is in the form of a mixing problem of a binary solution, but no extra term appears in Eq. (4.5), in contrast to Eq. (4.3). Note that only the occupation probabilities of individual sites are now encountered in the above equation; since there are two sites per bond, the free energy of the assembly is $\tilde{F}_{\alpha_1} = \frac{1}{2}\tilde{F}_{\beta_1}$, so that

$$\tilde{F}_{\alpha_1} = \varepsilon\psi + \varepsilon_{CA}/2 + k_B T\{\alpha_1 \ln \alpha_1 + (1 - \alpha_1)\ln(1 - \alpha_1)\}, \quad (4.6)$$

which quantity may be optimized by the requirement $\partial\tilde{F}_{\alpha_1}/\partial\alpha_1 = 0$. This leads to the equilibrium condition

$$\frac{\varepsilon(\psi) + \psi\,\varepsilon'(\psi)}{k_B T} = -\ln\left(\frac{\psi}{1 - \psi}\right). \quad (4.7)$$

(C) $C \rightarrow \infty$ under the sufficient condition that $\varepsilon \rightarrow \infty$. This situation is not of interest since it places the conduction states characterized by $\beta_1 = 0$ out of reach of the thermal population.

5. Discussion

As described in more detail elsewhere *(18, 19)*, we recover explicitly the results first derived by Strässler and Kittel (SK) *(20)* if we assume that ε is specified by the linear relation $\varepsilon(\psi) = \varepsilon_0 - \frac{1}{2}\lambda\psi$. In their framework first and second order transitions were treated in a single unified scheme, which leads to the following expression for the free energy:

$$F = (\varepsilon_0 - \tfrac{1}{2}\lambda\psi)\psi + k_B T[\psi \ln \psi + (1 - \psi)\ln(1 - \psi) - \psi \ln g_1 - (1 - \psi)\ln g_0]. \quad (5.1)$$

Here g_1 and g_0 are the degeneracies of a two-level system. The terms involving g_1 and g_0 were grafted onto a slightly modified version of the standard theory of mixing of a two-component solution. The application of Eq. (5.1) to magnetite was discussed in detail in earlier publications *(21, 22)*. To fit the data it was necessary to set $g_1 = 2g_0 = 2$ for stoichiometric magnetite, and to set $g_1 = g_0$ in the second-order regime, as demanded by the theoretical analysis *(20)* of Eq. (5.1). However, it was not clear at the time how the two-level scheme was related to the magnetite system.

In the present approach, the form of Eq. (5.1) is an automatic consequence of the order–disorder formalism. In particular, Eq. (4.3) corresponds with the expression (5.1) with $g_1 = 2g_0 = 2$; Eq. (4.4) serves as a means to determine ψ as a function of T by numerical techniques. The order parameter is found to exhibit a discontinuity at $T = T_V$. Similarly, Eq. (4.6) corresponds to (5.1) when one takes $g_1 = g_0 = 1$; the corresponding order parameter as calculated from Eq. (4.7) is continuous at $T = T_V$, but its first derivative is discontinuous.

The application of Eqs. (4.2)–(4.7) to the analysis of the experimental results in $Fe_{3(1-\delta)}O_4$ and in $Zn_xFe_{3-x}O_4$ has been described in detail in earlier publications *(16, 18, 21, 22)* and need not be repeated. The success of such a simple approach in confronting experimental thermodynamic and transport phenomena in the magnetite system shows that the present model serves as a useful starting point for a more sophisticated theory. It is planned to investigate less simplistic models in the future.

Acknowledgment

This research was supported by Grant DMR-89 21293 A01 of the National Science Foundation.

References

1. R. W. Millar, *J. Am. Chem. Soc.* **51,** 215 (1929).
2. E. J. W. Verwey, *Nature (London)* **144,** 327 (1989).
3. R. Dieckmann, *Ber. Bunsenges. Phys. Chem.* **86,** 112 (1982).
4. R. Dieckmann and H. Schmalzried, *Ber. Bunsenges. Phys. Chem.* **81,** 344 (1977); **81,** 414 (1977).
5. E. Gmelin, N. Lenge, and H. Kronmüller, *Phys. Status Solidi A* **79,** 465 (1983).
6. J. P. Shepherd, J. W. Koenitzer, C. J. Sandberg, R. Aragón, and J. M. Honig, *Mol. Cryst. Liq. Cryst.* **107,** 191 (1984).
7. R. Aragón, D. J. Buttrey, J. P. Shepherd, and J. M. Honig, *Phys. Rev. B* **31,** 430 (1985).
8. J. P. Shepherd, J. W. Koenitzer, R. Aragón, C. J. Sandberg, and J. M. Honig, *Phys. Rev. B* **31,** 1107 (1985).
9. R. Aragón, J. P. Shepherd, J. W. Koenitzer, D. J. Buttrey, R. J. Rasmussen, and J. M. Honig, *J. Appl. Phys.* **57,** 3221 (1985).

10. J. P. Shepherd, R. Aragón, J. W. Koenitzer, and J. M. Honig, *Phys. Rev. B* **32,** 1818 (1985).

11. R. Aragón, R. J. Rasmussen, J. P. Shepherd, J. W. Koenitzer, and J. M. Honig, *J. Magn. Magn. Mater.* **54–57**, 1335 (1986).

12. R. J. Rasmussen, R. Aragón, and J. M. Honig, *J. Appl. Phys.* **61,** 4395 (1987).

13. G. Haley, J. G. Mullen, and J. M. Honig, *Solid State Commun.* **69,** 285 (1989).

14. Z. Kąkol and J. M. Honig, *Phys. Rev. B* **40,** 9090 (1989).

15. P. Wang, Z. Kąkol, M. Wittenauer, and J. M. Honig, *Phys. Rev. B* **42,** 4553 (1990).

16. Z. Kąkol, J. Sabol, and J. M. Honig, *Phys. Rev. B* **43,** 649 (1991).

17. J. W. Koenitzer, Ph.D. Thesis, Purdue University, to be submitted.

18. J. M. Honig and J. Spałek, *J. Less-Common Metals* **156,** 423 (1989).

19. J. M. Honig, J. Spałek, and P. Gopalan, *J. Am. Ceram. Soc.* **73,** 3225 (1990).

20. S. Strässler and C. Kittel, *Phys. Rev.* **139,** A758 (1965).

21. R. Aragón and J. M. Honig, *Phys. Rev. B* **37,** 209 (1988).

22. J. M. Honig, *Phys. Chem. Miner.* **15,** 476 (1988).